Quadratic Chirp Modulation for Underwater Acoustic Digital Communications

Andrés Nicolás Carvallo Pecci, Christophe Laot, Arnaud Bourre

Quadratic Chirp Modulation for Underwater Acoustic Digital Communications

Andres CARVALLO PECCI
SC department, Telecom Bretagne
Institut Mines-Telecom,
UMR CNRS 6285 Lab-STICC
Brest, France
andres.carvallopecci@telecom-bretagne.eu

Christophe LAOT
SC department, Telecom Bretagne
Institut Mines-Telecom,
UMR CNRS 6285 Lab-STICC
Brest, France
christophe.laot@telecom-bretagne.eu

Arnaud BOURRE
DGA Ingénierie des Projets
Ministère de la défense
Bagneux, France
arnaud.bourre@intradef.gouv.fr

***Abstract*—A real demand for underwater acoustic (UWA) communications exists in oceanography, ocean exploration and undersea navigation. A new Doppler resilient digital communication, based on quadratic frequency modulations (QFM) is presented. The binary information is transmitted using two orthogonal QFM chirps. This signal modulation is suitable for low-data-rate communication such as telemetry. The first motivation of this paper resides in the performance of the non-coherent detector for binary QFM signal detection. It is shown that for some spreading factors, the detection of QFM signal waveform gives better performance than a linear frequency modulation (LFM) signal waveform in terms of bit error rate. The second motivation is that the non-coherent receiver is more Doppler resilient for QFM waveforms than LFM. An analytical demonstration is given, which predicts the simulated results. Real underwater commutations were accomplished on the Atlantic Ocean on February 2015.**

Keywords—Linear & Quadratic Frequency Modulation (LFM & QFM); Doppler compression-dilatation; Non-coherent detection; Underwater acoustic (UWA) channel.

I. INTRODUCTION

Digital communications have evolved to the point it is possible to communicate underwater. When studying the problem of sending information form one point to another, the perturbations induced by the channel must be analyzed, for then being able to choose a proper signal waveform.

Reliable UWA communications is challenging due to the channels' characteristics. These include high power attenuation, small bandwidth, fast time variability, signal compression-dilatation due to relative speed between source and receiver and multi-path propagation.

The low celerity of acoustic waves results in larger Doppler shifts than in radio transmissions. This is not the only effect of Doppler in acoustic waves. Unlike radio waves, which Doppler shift is modelled as a frequency offset, symbol duration compression dilatation cannot be neglected. If the Doppler is significant, this results on frame desynchronization and loss of information. Relative speed between source and receiver is not the only cause of signal compression-dilatation. Difference between the sampling frequencies has the same consequence as Doppler. This means that if digital-analog-converter is not accurate, we have to take into account this problem in our system.

Coherent modulation methods have been extensively studied during the past years. These methods have good spectral efficiency, however in practice, when communication robustness is desired above bit rate, non-coherent modulations are favored. A non-coherent modulation will be presented as shown in Fig. 1. This means that there will be two signals representing the bits, and we will do the projection of the observation on the respective signals subspaces and compare the energy of both projections to see which is bigger. An intuitive consideration is that if the signals are orthogonal, the system performance will increase.

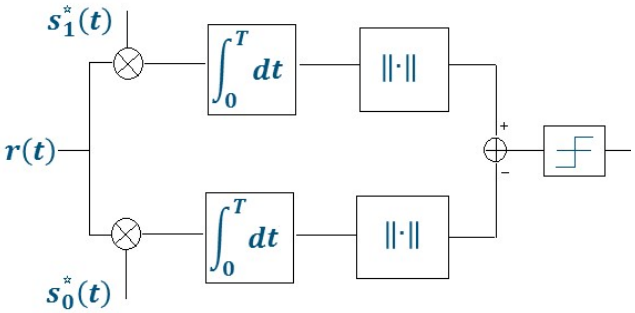

Fig. 1. Non-coherent detector block diagram.

Chirp spread spectrum (CSS) techniques seem to be reliable, given their low Doppler sensitivity and multipath robustness as presented in [1]-[7]. The first chirp waveform that comes to mind is the linear frequency modulation (LFM) because of its simplicity. The problem of this waveform is that to obtain orthogonality between two LFM, large time-frequency product (also known as spreading factor) are needed as shown in [8]. Large spreading factors will mean considerable symbol periods or wide bandwidths. Ideally, we are interested in having significant bit rates while keeping good robustness properties. Thus, a LFM will occupy undesirable large bandwidths. Nevertheless, it could be possible to do digital signaling with non-orthogonal LFM with small spreading factors, but it will not be an optimal waveform in the sense of minimizing errors.

Therefore, it is important to decide which chirp signal will be sufficiently orthogonal for small spread factors to send information. In this paper, it will be analyzed the quadratic frequency modulation (QFM) as shown in Fig. 2.

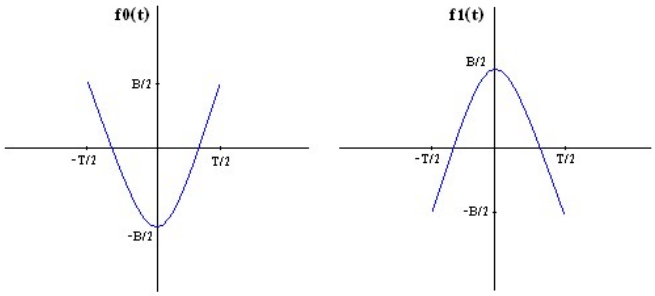

Fig. 2. Instantaneous frequency of binary QFM

LFM are widely used in radar applications for its resilience to Doppler as indicated in [9]. Its ambiguity function has been deeply studied to prove its correlation properties face severe Doppler. An important property of QFM is that it is more resilient to Doppler than LFM waveforms as shown in [10].

II. System Model

We will start by expressing mathematically the signal waveforms, and then express mathematically the effect on the signal of a compression-dilatation.

A. LFM and QFM

LFM is the first and probably still is the most popular frequency modulation. It was conceived during World War II, independently on United States and Europe for radar applications. Our application is not distant from a detection problem such as in radar or sonar. Here, LFM is used to perform a digital communication. Considering an up-LFM and down-LFM as

$$s_0(t) = \begin{cases} Re\left\{\sqrt{\frac{2\varepsilon_b}{T}} e^{j2\pi\left(f_c t + \frac{B}{2T}t^2\right)}\right\}, & -\frac{T}{2} < t < \frac{T}{2} \\ 0, & otherwise \end{cases} \quad (1)$$

$$s_1(t) = \begin{cases} Re\left\{\sqrt{\frac{2\varepsilon_b}{T}} e^{j2\pi\left(f_c t - \frac{B}{2T}t^2\right)}\right\}, & -\frac{T}{2} < t < \frac{T}{2} \\ 0, & otherwise \end{cases} \quad (2)$$

where ε_b is the signal energy, T is the time period, B is the bandwidth and f_c is the carrier frequency. The spreading factor will be defined as the product of the bandwidth and time period BT. This parameter expresses the spreading of the signal over the time-frequency space. In this paper a constant signal envelope is considered. Assuming a non-constant signal envelope changes the signal's correlation and orthogonality properties, which is beyond the objective of this paper.

We will use s_0 and $s_1$to code a bit 0 and 1 respectively. The hypothesis test is presented as follows

$$\begin{cases} H_0 : r = s_0 + n \\ H_1 : r = s_1 + n \end{cases} \quad (3)$$

Where $n \sim N(0, \frac{N_0}{2})$ is an additive Gaussian white noise (AWGN). Given the structure of the non-coherent maximum a posteriori detector, deciding H_1 (a bit equal to 1) or H_0 (a bit equal to 0)

$$\|\langle r, s_1\rangle\| - \|\langle r, s_0\rangle\| \underset{H_0}{\overset{H_1}{\gtrless}} 0 \quad (4)$$

Where $\|\langle *, *\rangle\|$ is the absolute value of the scalar product between the observation r and s_1 and s_0 respectively. Considering choosing H_1 knowing H_0 occurs (which means an error happens),

$$\|\langle s_0, s_1\rangle + \langle n, s_1\rangle\| - \|\langle s_0, s_0\rangle + \langle n, s_0\rangle\| > 0 \quad (5)$$

Analyzing expression (5), given that for LFM signals $\langle s_0, s_1\rangle \neq 0$ the performance will deteriorate in terms of bit error rate in comparison to the case when the waveforms are orthogonal.

QFM signals have an instantaneous frequency as shown in Fig. 2. This can be expressed mathematically as

$$s_0(t) = \begin{cases} Re\left\{\sqrt{\frac{2\varepsilon_b}{T}} e^{j2\pi\left((f_c - \frac{B}{2})t + \frac{4B}{3T^2}t^3\right)}\right\}, & -\frac{T}{2} < t < \frac{T}{2} \\ 0, & otherwise \end{cases} \quad (6)$$

$$s_1(t) = \begin{cases} Re\left\{\sqrt{\frac{2\varepsilon_b}{T}} e^{j2\pi\left((f_c + \frac{B}{2})t - \frac{4B}{3T^2}t^3\right)}\right\}, & -\frac{T}{2} < t < \frac{T}{2} \\ 0, & otherwise \end{cases} \quad (7)$$

In section III we will study the orthogonality of the QFM to show the first interest of using this waveform.

B. Doppler compression-dilatation

As the receiver and transmitter move with relative speed v the waveform suffers a compression-dilatation [12], which could be modeled as follows

$$s_d(t) = s_i\left(t\left(1 - \frac{v}{c}\right)\right);\ i = 0,1 \quad (8)$$

where c is the celerity of acoustic waves in sea water. For the LFM this effect could be expressed as

$$s_d(t) = \begin{cases} Re\left\{\sqrt{\frac{2\varepsilon_b}{T}} e^{j2\pi\left(f_c\left(1-\frac{v}{c}\right)t \pm \frac{B}{2T}\left(1-\frac{v}{c}\right)^2 t^2\right)}\right\}, & -\frac{T\left(1-\frac{v}{c}\right)}{2} < t < \frac{T\left(1-\frac{v}{c}\right)}{2} \\ 0, & otherwise \end{cases} \quad (9)$$

The effect of the compression-dilatation will impact on the waveform in two ways, a Doppler frequency shift that is proportional to the carrier frequency $\Delta f_d = \frac{v}{c} f_c$. This term also exists when we work with radio waves, even though the celerity of radio waves is several orders of magnitude greater than acoustic waves.

The second impact of the Doppler compression-dilatation is the term $\frac{B}{2T}\left(1 - \frac{v}{c}\right)^2$. The $\left(1 - \frac{v}{c}\right)^2$ factor will change the slope of the linear chirp. The term $\frac{B}{2T}\left(1 - \frac{v}{c}\right)^2$ is related to the waveforms robustness to Doppler. If $\frac{B}{T} \to +\infty$ the slope of the LFM will remain unchanged by Doppler.

For the QFM a similar expression of the Doppler compression-dilatation as the one shown in (9) is the following

$$s_d(t) = s_i\left(t\left(1-\frac{v}{c}\right)\right) = \begin{cases} Re\left\{\sqrt{\frac{2\varepsilon_b}{T}}e^{j2\pi\left((f_c\mp\frac{B}{2})\left(1-\frac{v}{c}\right)t\pm\frac{4B}{3T^2}\left(1-\frac{v}{c}\right)^3t^3\right)}\right\}, & -\frac{T\left(1-\frac{v}{c}\right)}{2} < t < \frac{T\left(1-\frac{v}{c}\right)}{2} \\ 0, & otherwise \end{cases} \quad (10)$$

Once again, a Doppler frequency shift proportional to $\Delta f_d \cong \frac{v}{c}f_c$ (considering $B \ll f_c$) and the term $\frac{4B}{3T^2}\left(1-\frac{v}{c}\right)^3$ related to the Doppler resilience.

III. Orthogonality & Doppler Resilience

We will start discussing the orthogonality of both LFM and QFM and compare them as a function of the spread factor BT and then we will talk over the Doppler resilience of both waveforms.

A. Orthogonality

Considering the orthogonality between two waveforms as

$$\langle s_0, s_1\rangle = \int_{-T/2}^{T/2} s_0(t)s_1^*(t)dt \quad (11)$$

Without loss of generality, for calculating $\langle s_0, s_1\rangle$ we use the complex expressions of s_0 and s_1.

For the LFM, the cross inner product becomes

$$\langle s_0, s_1\rangle = \frac{2\varepsilon_b}{T}\int_{-\frac{T}{2}}^{\frac{T}{2}} e^{j2\pi\frac{B}{T}t^2}dt = \frac{4\varepsilon_b}{\sqrt{2\pi BT}}\left[C\left(\frac{1}{2}\sqrt{2\pi BT}\right)+jS\left(\frac{1}{2}\sqrt{2\pi BT}\right)\right] \quad (12)$$

Where $C(x)$ and $S(x)$ are the cosine and sine Fresnel integrals defined as

$$C(x) = \int_0^x \cos(t^2)dt \;;\; S(x) = \int_0^x \sin(t^2)dt \quad (13)$$

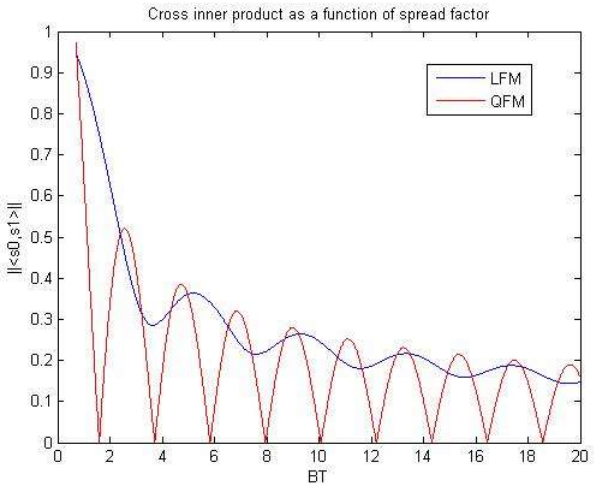

Fig. 3. Cross inner product for LFM and QFM

We observe that $\|\langle s_0, s_1\rangle\|$ tends to zero when $BT \to +\infty$. For the QFM we find

$$\langle s_0, s_1\rangle = \frac{2\varepsilon_b}{T}\int_{-T/2}^{T/2} e^{j2\pi\left(-Bt+\frac{8B}{3T^2}t^3\right)}dt \quad (14)$$

To solve the integral we will use the stationary-phase approximation [10] which gives us

$$\|\langle s_0, s_1\rangle\| \cong \frac{\varepsilon_b}{\sqrt{\sqrt{2}BT}}cos\left(2\pi\left(\frac{\sqrt{2}BT}{6}-\frac{1}{8}\right)\right) \;;\; \frac{B}{T}\to\infty \quad (15)$$

Fig. 3 shows the cross inner product $\|\langle s_0, s_1\rangle\|$ of the LFM waveform (12) and the QFM cross inner product approximation (15) as a function of BT. Both waveforms decay proportional to $\frac{1}{\sqrt{BT}}$. The QFM cross inner product is a periodic function of BT, which means that for certain spreading factors it is orthogonal.

B. Doppler Resilience

We will now study the Doppler resilience for both waveforms. The ambiguity function has been widely used, especially in radar [9-11], to study the properties of waveforms with respect to time-frequency shifts. In our case, we work with a different version of the ambiguity function than the commonly used in radar. The ambiguity function is defined as follows

$$\Lambda_i(\tau, v) = \int_{-\infty}^{+\infty} s_i\left(t\left(1-\frac{v}{c}\right)\right)s_i{}^*(t-\tau)dt; i = 0,1 \quad (16)$$

Defining the cross-ambiguity function as

$$\Lambda_{i,j}(\tau, v) = \int_{-\infty}^{+\infty} s_i\left(t\left(1-\frac{v}{c}\right)\right)s_j{}^*(t-\tau)dt; i \neq j \quad (17)$$

To study the Doppler robustness of the non-coherent detector, we will look at the difference between the ambiguity function and the cross-ambiguity function

$$\Gamma(\tau, v) = \|\Lambda_i(\tau, v)\| - \left\|\Lambda_{i,j}(\tau, v)\right\|; i = 0,1 \quad (18)$$

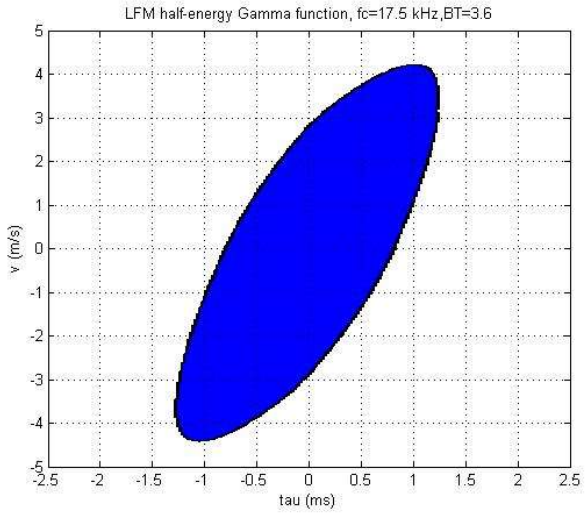

Fig. 4. LFM half-energy contour, $fc = 17.5$ kHz, BT 3.6 and $T = 10$ ms

On Fig. 4 and Fig. 5, we define a half-energy contour, which are all the points τ, v that $\Gamma(\tau, v) > \frac{\varepsilon_b}{2}$.

The carrier frequency was chosen with respect to the transducer used on the trials, and the spreading factor is the second root of the QFM cross inner product function as shown in Fig. 3.

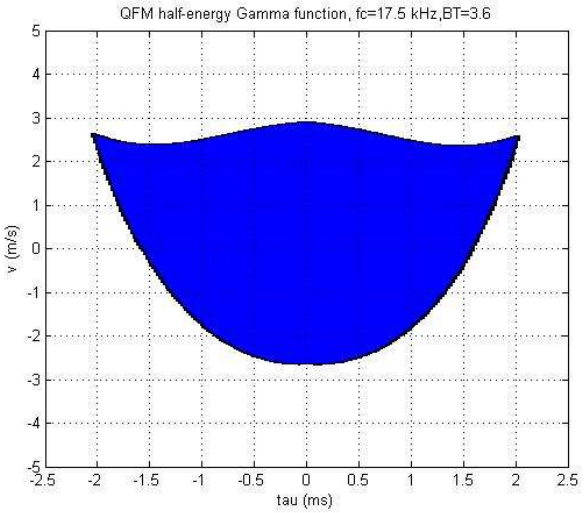

Fig. 5. QFM half-energy contour, $fc = 17.5$ kHz, $BT = 3.6$ and $T = 10$ ms

Fig. 4 and Fig.5 give an idea of the robustness to an error in synchronization and the robustness to a relative speed between source and receiver. As the area of the QFM half-energy contour is bigger than the LFM's, it can be deduced that it is more resilient to Doppler and to a synchronization error.

Fig. 6 and Fig. 7 show the 70 % energy contour of LFM and QFM respectively.

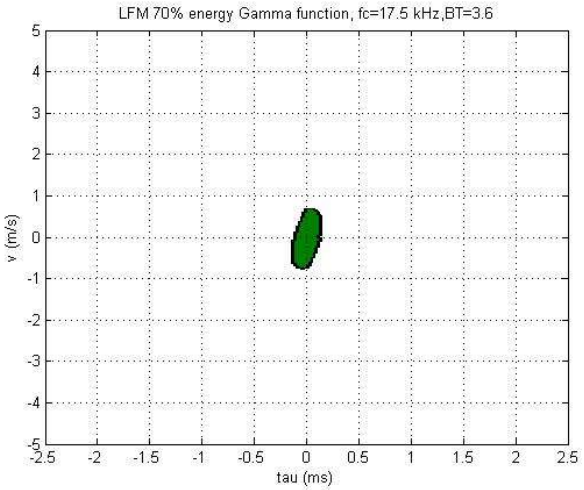

Fig. 6. LFM 70% energy contour, $fc = 17.5$ kHz, $BT = 3.6$ and $T = 10$ ms

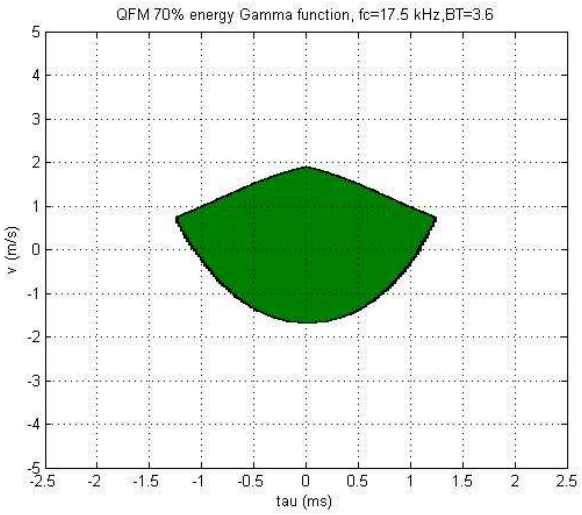

Fig. 7. QFM 70% energy contour, $fc = 17.5$ kHz, $BT = 3.6$ and $T = 10$ ms

On these figures we observe the effect of the non-orthogonality of the LFM given that the contour's area is heavily reduced.

It is interesting to highlight that for some cases, the $\Gamma(\tau, v)$ function is negative, which means that for those values of τ, v the decision will be inverted. Fig. 8 and Fig. 9 show the $\Gamma(\tau, v)$ contour for negative values.

This means that for the light green regions there will be errors in every bit even in the absence of noise.

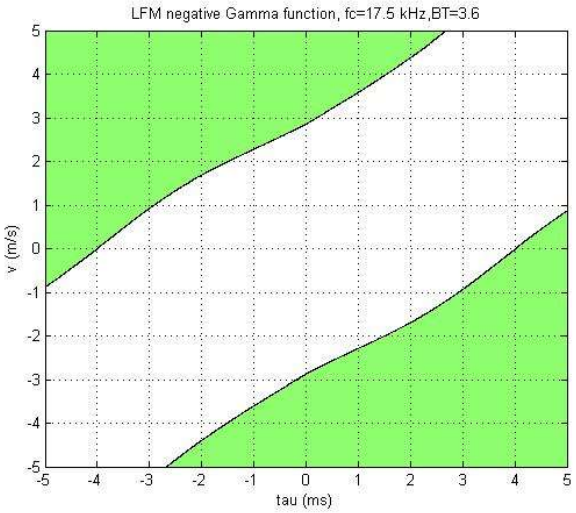

Fig. 8. LFM negative contour, $fc = 17.5$ kHz, $BT = 3.6$ and $T = 20$ ms

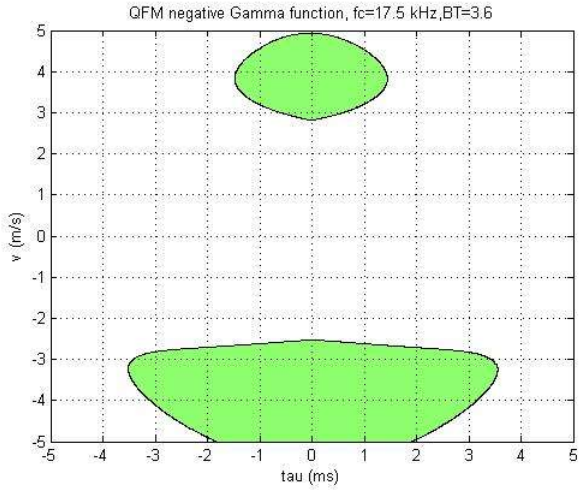

Fig. 9. QFM negative contour, $fc = 17.5$ kHz, $BT = 3.6$ and $T = 20$ ms

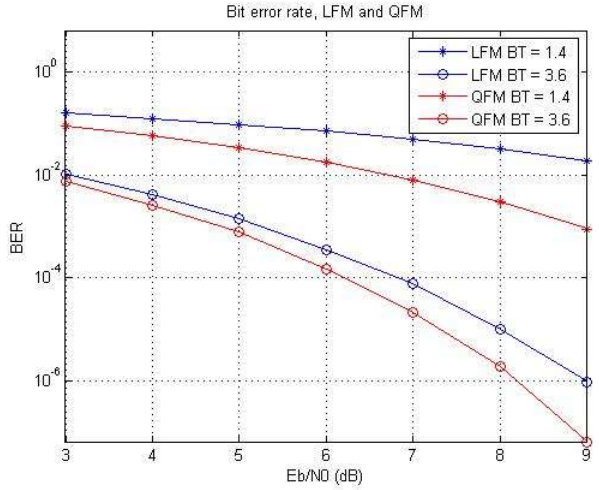

Fig. 10. LFM and QFM Bit error rate, $BT = 1.4$

IV. Simulation ans Results

To illustrate the results, we will begin showing the performance of LFM and QFM over a noisy channel. Next, we show the behavior of the detector with Doppler and noise simultaneously. Finally, we will present the results obtained over a real underwater channel.

A. Noisy Channel

Considering the test hypothesis (3), the non-coherent detector is

$$\|\langle r, s_1\rangle\| - \|\langle r, s_0\rangle\| \underset{H_0}{\overset{H_1}{\gtrless}} 0 \tag{19}$$

As $n \sim N\left(0, \frac{N_0}{2}\right)$ and assuming H_0 was transmitted, we find

$$\langle s_0 + n, s_0\rangle \sim N\left(\varepsilon_b, \frac{\varepsilon_b N_0}{2}\right);\ \langle s_0 + n, s_1\rangle \sim N(\varepsilon_{01}, \frac{\varepsilon_b N_0}{2}) \tag{20}$$

As $\|\langle r, s_0\rangle\|$ is the absolute value of a non-centered Gaussian variable, $\|\langle r, s_1\rangle\| - \|\langle r, s_0\rangle\|$ is the subtraction of two Rice distributions.

We will not go into further detail of the theoretical bit error probability, we will only highlight that a non-coherent detector has slightly lower performance than the coherent detector. The reason we chose a non-coherent detector is that it is easier to synchronize, because there is no need to estimate the phase. Phase estimation sometimes requires advanced signal processing such as phase-lock loop (PLL). Avoiding this kind of problem with a non-coherent detector seems interesting.

Fig. 10 shows the simulated bit-error rate of the LFM and QFM non-coherent detector. We used a spread factors $BT = 1.4$ and 3.6. This values where chosen because as shows Fig. 3, they are the first and second roots of the QFM cross inner product function, which means that the QFM waveforms are orthogonal for these values.

We observe lower bit error rate for the QFM than for LFM at same BT. For $BT = 1.4$, the difference between the LFM and QFM BER is higher than for $BT = 3.6$. This is because the difference of cross-inner product as shown in Fig. 3 is greater for $BT = 1.4$ than for $BT = 3.6$.

B. Doppler Channel.

The simulated performance of the detector over a Doppler and noisy channel are shown in this section. It must be highlighted that there are several parameters that count when introducing Doppler into the channel. The carrier frequency will have an important impact in the performances given that the Doppler frequency shift is $\Delta f_d \cong \frac{v}{c} f_c$. If the Doppler frequency shift is significant over the bandwidth, the bit error rate risks being poor.

For the simulations, it was used a carrier frequency of $f_c = 17.5$ kHz and a relative speed $v = 1\ m/s$. Fig. 11 shows the results for these values.

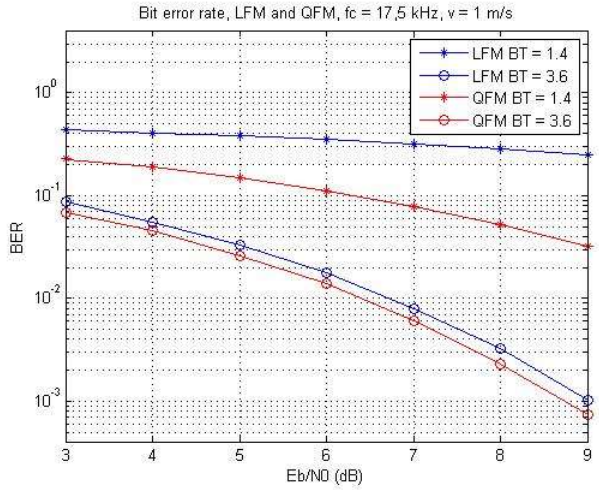

Fig. 11. LFM and QFM BER, $f_c = 17.5$ kHz and $v = 1$ m/s

The performance is deteriorated with respect to the noisy channel of section IV.A. This is because of the Doppler. The Doppler frequency shift is $\Delta f_d = \frac{v}{c} f_c = 11{,}6$ Hz and the bandwidth are $B_{@1.4} = 140$ Hz and $B_{@3.6} = 360$ Hz, which makes the ratio frequency shift over bandwidth less than $\frac{\Delta f_d}{B} < 10\%$. Nevertheless, the performance is superior with the QFM waveform.

C. Real UWA channel.

We had the opportunity to organize real trials in the Atlantic Ocean on February 2015. The trials where done between docks in the port of Brest, Brittany, France as shown in Fig. 12 at a distance of $d = 800$ m.

For the trials, it was used a spherical omnidirectional transducer ITC-1001 with a resonance frequency $f_r = 17.5$ kHz and a transmitting voltage response $TVR = 149$ dB/µPa/V @ 1m. Given the resonance frequency we chose a carrier frequency $f_c = 17.5$ kHz.

In reception, 4 hydrophones Brüel & Kjaer types 8106 were used and two National Instruments cards (NI-USB 6356) as DA/AD converters,

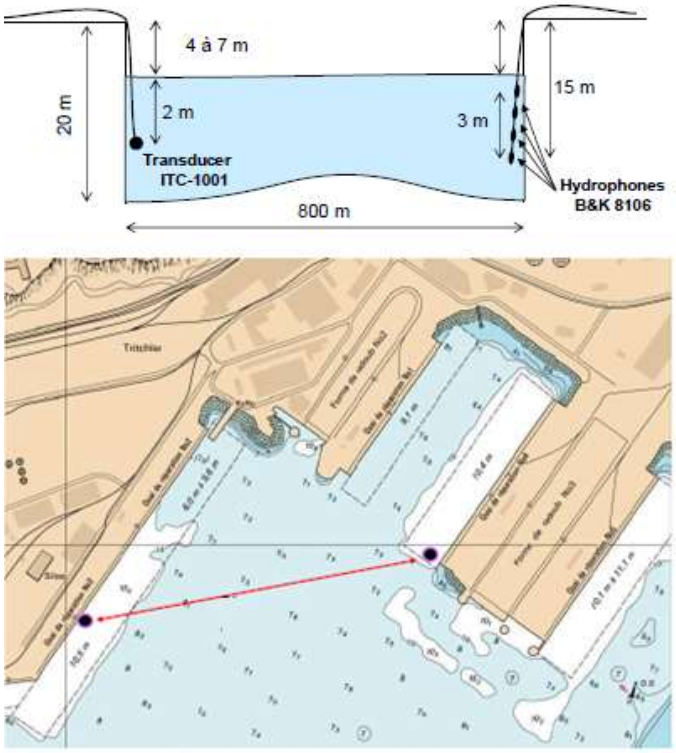

Fig. 12. Real trials, transmission setup.

It is shown in table 1, the results obtained from the trials. The transmission were done for different time periods $T = 5, 10$ and 20 ms. We send approximately 5000 bits of information with a spreading factor $BT = 1.4$ for the QFM and $BT = 3.6$ for both LFM and QFM. We used a band of $3\ kHz$ where we multiplexed several LFM and QFM waveforms on the whole band. Frames of 250 ms were used, synchronized by a pilot signal at the beginning of the frame. Each frame contained 240 bits/frame when $BT = 1.4$ and 96 bits/frame when $BT = 3.6$.

In reception we had 4 hydrophones, hence we have 4 BER estimate each time on Table 1 and Table 2.

The SNR varies between $4 - 25dB$ depending on the hydrophone and on the frame, consequently sometimes we have high BER.

LFM			QFM		
T (ms)	*Hydrophone*	*BER*	*T (ms)*	*Hydrophone*	*BER*
5	1	0,09	5	1	0,1
	2	0,02		2	0,05
	3	0,01		3	0,04
	4	0,01		4	0,002
10	1	0,04	10	1	0,1
	2	0,02		2	0,005
	3	0,04		3	0,02
	4	0,0001		4	0,005
20	1	0,08	20	1	0,04
	2	0,01		2	0
	3	0,01		3	0,01
	4	0,007		4	0

Table 1. LFM and QFM BER, real UWA trials $BT = 3.6$

In general the QFM performed better than the LFM. Table 2 shows the results of QFM for a spreading factor $BT = 1.4$

QFM			
BT	*T (ms)*	*Hydrophone*	*BER*
1,4	5	1	0,41
		2	0,1
		3	0,06
		4	0,03
	10	1	0,3
		2	0,1
		3	0,06
		4	0,003
	20	1	0,28
		2	0,1
		3	0,06
		4	0,003

Table 2. QFM BER, real UWA trials $BT = 1.4$

We observe that even at a low spreading factor, when signal to noise ratio is sufficient, we arrive to send information with acceptable BER which could be decreased using channel coding. The using of this low spreading factor would not have been possible with the LFM waveform.

It must be underlined that given the difference between the sampling frequencies, we have done a frequency sampling compensation for decoding the information.

V. CONCLUSION

A Doppler resistant way of sending information with quadratic chirps is studied in this paper. This waveform was compared analytically and in simulation with a classic linear frequency modulation and showed that it performs better in presence of noise and Doppler. Its implementation for telemetry has been justified assuming the difficulty of sending small duration bursts.

It must be highlighted that the LFM and QFM studied on this paper have constant instantaneous amplitude. Orthogonality and correlation properties will change if we change the signal's envelope. Additionally, it may be interesting to analysis these properties in the future.

Further analysis would include the investigation of the waveform's robustness to multi-path propagation.

REFERENCES

[1] M. R. Winklern, "Chirp signals for communications" *IEEE WESCON*, 1962.

[2] D. S. Dayton and W. H. Smith A, "FM chirp communications: An easily-instrumented multiple access modulation form for dispersive channels", *IEEE Int. Conf. Communications*, 1967.

[3] A. Berni and W. Gregg, "On the utility of chirp modulation for digital signalling", *IEEE Trans. Commun*., vol. 21, no. 6, pp.748 -751 1973.

[4] S. Hengstler, D. P. Kasilingam and A. H. Costa, "A novel chirp modulation spread spectrum technique for multiple access", *Proc. 7th IEEE Int. Symp. Spread Spectrum Techniques Applications*, vol. 1, pp.73 -77, 2002.

[5] C. He, J. Huang, and Q. Zhang, "M-ary chirp spread spectrum modulation for underwater acoustic communication," in *Proc. IEEE Tencon'05*, Austrial, Sept. 2005.

[6] C. He, J. Huang, Q. Zhang and K. Lei, "Reliable Mobile Underwater Wireless communication using wideband chirp signal", *IEEE International conference on communications and mobile computing*, 2009.

[7] C. He, M. Ran, Q. Meng and J. Huang, "Underwater Acoustic Communications using M-ary Chirp-DPSK Modulation", *IEEE 10th International Conference on Signal Processing (ICSP)*, 24-28 Oct. 2010.

[8] Q. Wang and J. Jiang, "Performances of trigonometric chirp spread spectrum modulation in AWGN & Rayleigh channels", *PM2HW2N'13*, Barcelona, Spain Nov. 3-8, 2013.

[9] N. Levanon. Radar Principles. John Wiley and Sons, 1988.

[10] R. Diamanat, A. Feuer, and L. Lampe, "Choosing the right signal: Doppler shift estimation for underwater acoustic signals," in *WUWNet12*, Los Angeles, CA, USA, Nov. 5–6, 2012.

[11] Skolnik, M I. Radar handbook, McGraw-Hill, 1970

[12] B. S. Sharif, J. Heasham, O. R. Hinton, A. E. Adams, "A Computationally Efficient Doppler Compensation System for Underwater Acoustic Communications." *IEEE Journal of oceanic engineering*, vol. 25, no. 1, Jan. 2000